

CHANDRA DETECTION OF A CLOSE X-RAY COMPANION AND RICH EMISSION-LINE SPECTRUM IN THE WOLF-RAYET BINARY γ VELORUM

STEPHEN L. SKINNER

Center for Astrophysics and Space Astronomy, University of Colorado, Campus Box 389, Boulder, CO 80309-0389

MANUEL GÜDEL

Paul Scherrer Institute, Würenlingen and Villigen, CH-5235, Switzerland

WERNER SCHMUTZ

Physikalisch-Meteorologisches Observatorium Davos, Dorfstrasse 33, CH-7260 Davos Dorf, Switzerland

AND

IAN R. STEVENS

School of Physics and Astronomy, University of Birmingham, Birmingham B15 2TT, UK

Received 2001 May 16; accepted 2001 July 30; published 2001 August 23

ABSTRACT

We present first results of a high-resolution X-ray observation of the nearby Wolf-Rayet binary system γ^2 Velorum (WC8 + O7.5) using the *Chandra* High-Energy Transmission Grating (HETG). Emission lines from Mg, Si, S, Ne, and Fe dominate the spectrum and imply a range of plasma temperatures from ~ 4 MK up to at least ~ 25 MK. The strongest lines are broadened, but no Doppler shifts are detected. He-like triplets show strong forbidden lines with no significant weakening from collisional effects or photoexcitation, contrasting sharply with the diluted forbidden lines of single O-type supergiants such as ζ Puppis. These results imply that some lines such as the Ne IX triplet are formed in cooler plasma at tens of stellar radii or more from the O star, well outside of the central wind interaction region located near the O star surface. Lastly, we report the discovery of a new X-ray source lying only $4''.8$ north of γ^2 Vel that is very likely a low-mass pre-main-sequence star.

Subject headings: stars: individual (γ^2 Velorum, HD 68273) — stars: Wolf-Rayet — X-rays: stars

1. INTRODUCTION

The origin of X-ray emission from massive OB and Wolf-Rayet (W-R) stars is a fundamental unanswered question in stellar astrophysics. In massive single stars without companions, the X-rays are thought to arise in radiative shocks that form in the outer wind as a result of line-driven instabilities (Lucy & White 1980). Radiative shock emission is expected to be soft and weakly absorbed, and this mechanism appears to be consistent with *Chandra* and *XMM-Newton* grating spectra of the O4 Ief supergiant ζ Puppis (Cassinelli et al. 2001; Kahn et al. 2001). However, hot plasma confined in magnetic loops near the stellar surface may also play a role, as proposed by Waldron & Cassinelli (2001) in their analysis of *Chandra* grating spectra of the O9 supergiant ζ Orionis.

The X-ray emission of massive binaries such as the W-R + O system γ^2 Velorum discussed here is potentially more complex since it may be the superposition of separate contributions from the individual stars and a colliding wind shock between the two stars (Prilutskii & Usov 1976; Usov 1992). The intrinsic X-ray properties of a colliding wind shock are primarily determined by the stellar mass-loss parameters and stellar separation. In general, colliding wind shock emission is expected to be harder than that of radiative shocks with maximum temperatures of several keV accompanied by heavy wind absorption. Previous *ROSAT* and *ASCA* observations of γ^2 Vel detected hot plasma ($kT \gtrsim 1$ keV) and strong orbitally phased absorption, which were interpreted as evidence for colliding wind shock emission (Willis, Schild, & Stevens 1995; Stevens et al. 1996).

We present initial results of *Chandra* observations of γ^2 Vel acquired at nearly the same orbital phase as the previous *ASCA* observations. γ^2 Vel (WC8 + O7.5) is a key system for testing theories of X-ray emission in massive binaries since it harbors the closest known W-R star at a *Hipparcos* distance of 258 pc (van der Hucht et al. 1997; Schaerer, Schmutz, & Grenon 1997).

Its orbit is well determined with $P_{\text{orb}} = 78.53$ days, $i = 63^\circ$, and $e = 0.326$ (Schmutz et al. 1997; De Marco & Schmutz 1999). The momentum of the W-R wind is dominant with $(Mv_\infty)_{\text{W-R}}/(Mv_\infty)_O \approx 33$ (De Marco et al. 2000). At the phases considered here, the hottest plasma from a colliding wind shock is predicted to form near the line of centers at a distance of at most $\sim 2 \times 10^{12}$ cm [$\sim 2R(O)$] from the O star. The *Chandra* spectra show that some of the X-rays originate at much larger distances.

2. CHANDRA OBSERVATIONS AND DATA REDUCTION

The observation began on 2000 March 15 at 09:20 UT and spanned 18.8 hr, giving a usable exposure of 64,848 s. It covered orbital phases $\phi = 0.076$ – 0.086 where $\phi = 0$ corresponds to periastron (Schmutz et al. 1997). The observation occurred 6 days after periastron and about 4 days after the passage of the O star in front of the W-R star ($\phi = 0.03$), at a stellar separation of ≈ 0.92 AU.

Grating spectra were obtained with the High-Energy Transmission Grating (HETG) using the six-chip ACIS-S detector in timed event mode. The HETG gives separate spectra from the medium-energy grating (MEG) and the high-energy grating (HEG). The HEG provides higher spectral resolution ($\Delta\lambda = 12$ mÅ FWHM, 1.2–15 Å) than the MEG ($\Delta\lambda = 23$ mÅ, 2.5–31 Å). However, the MEG gives a higher signal-to-noise ratio (S/N) in first-order spectra for γ^2 Vel. After combining data from +1 and –1 orders, we obtained 15,626 net counts in the MEG spectrum and 7626 net counts in the HEG spectrum.

Data reduction used products from *Chandra* X-Ray Center (CXC) first-phase reprocessing (Evans 2001) and followed CXC guidelines using CIAO v2.0.1, including the removal of weak field sources and background subtraction. Analysis was undertaken with Sherpa, HEASOFT version 5, and the Astro-

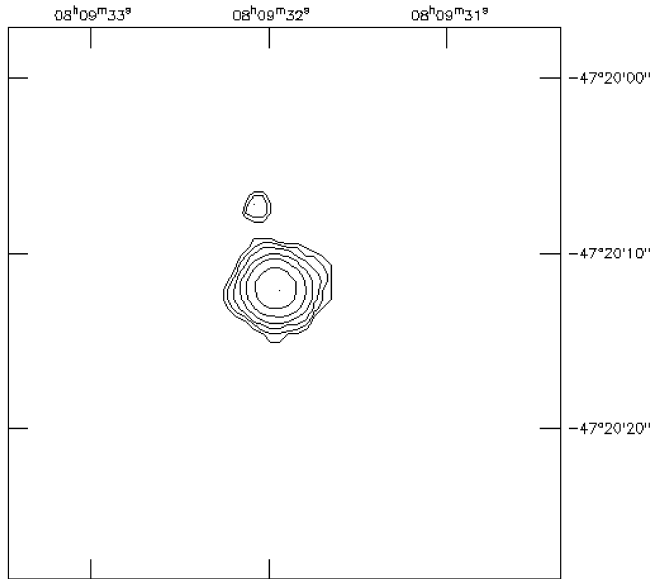


FIG. 1.—ACIS-S smoothed zeroth-order image (chip S3) for the region within 15'' of γ^2 Vel.

physical Plasma Emission Database (APED) as implemented in ATOMDB version 1.0.1 (Smith & Brickhouse 2000).

3. RESULTS

3.1. Images: A Double X-Ray Source

The ACIS-S zeroth-order contour image in Figure 1 shows strong emission from γ^2 Vel and the surprising detection of a weak source located 4".8 to its north (position angle [P.A.] = 8°). The image gives 10,038 counts (piled) from γ^2 Vel in zeroth order, but only 60 counts from the weaker source (9×10^{-4} counts s^{-1}). The weaker source has not been detected previously in X-rays and very likely corresponds to the IR source seen at nearly the same relative position (offset 4".72, P.A. = 13°3, $K = 13.4$) by Tokovinin et al. (1999), who classified it as a K4 V dwarf slightly above the main sequence. The presence of an X-ray source within 5'' of γ^2 Vel that may be a low-mass pre-main-sequence (PMS) star would be of considerable interest from the standpoint of stellar evolution and star formation theories if the two objects are found to be physically associated. This possibility warrants further investigation given the young age of the O star in γ^2 Vel (3.6 Myr; De Marco & Schmutz 1999) and the *ROSAT* evidence for a larger population of low-mass PMS stars surrounding γ^2 Vel (Pozzo et al. 2000).

3.2. Timing Analysis

We find no evidence for significant X-ray variability ($\geq 3\sigma$) in γ^2 Vel. Unpiled light curves were constructed using dispersed MEG photons (first order). A bin size of 256 s gives ≥ 60 counts per bin with a probability of constant count rate $P(\text{const}) = 0.993$ ($\chi^2/\text{degrees of freedom} = 203.6/256$).

3.3. Grating Spectra

3.3.1. General Properties

Figure 2 shows the first-order MEG spectrum with +1 and -1 orders combined. It is dominated by strong emission lines from Si, S, and Mg with many weaker lines from Fe and Ne. The strongest line is the Si XIII resonance line at 6.648 Å

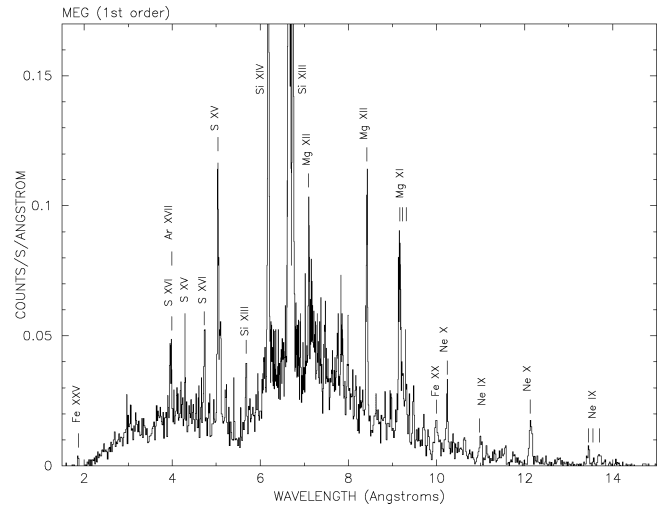


FIG. 2.—Background-subtracted MEG first-order spectrum binned at 0.02 Å

(Fig. 3). A broad range of plasma temperatures from ~ 4 MK up to at least ~ 25 MK is inferred from a comparison of the detected lines with their maximum emission temperatures (T_{max}) given in the APED. Cooler lines such as Ne IX (11.00 Å, $T_{\text{max}} = 4$ MK) are present as well as hotter lines such as S XVI (4.73 Å, $T_{\text{max}} = 25$ MK) and weak emission from the Fe K complex at 1.86 Å ($T_{\text{max}} = 40$ MK). Very little flux is detected above ~ 15 Å due to heavy wind absorption. Thus, low-energy C, N, and O lines are not accessible, and the distribution of plasma at temperatures below ~ 4 MK is not well determined. An underlying continuum is detected. Specifically, the total MEG count rate (source + background) in line-free intervals 3.22–3.36 Å and 4.43–4.70 Å is a factor of ~ 40 –100 greater than measured in the adjacent background.

We used an absorbed Chebyshev polynomial differential emission measure (DEM) model to estimate the broadband flux. At the phase of our observation, the O star is nearly in front of the W-R star, and we thus assume that the absorption is due

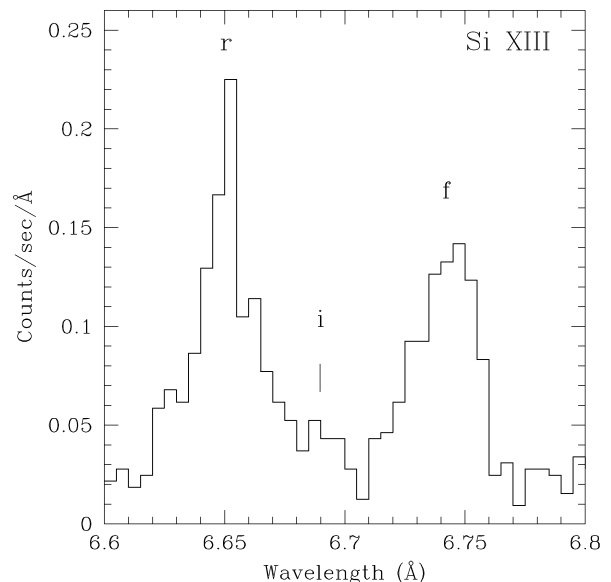


FIG. 3.—Si XIII triplet in HEG first-order binned at 0.005 Å, where *r*, *i*, and *f* mark the resonance, intercombination, and forbidden lines.

TABLE 1
 γ^2 VEL EMISSION-LINE PROPERTIES

Parameter	Ne IX	Mg XI	Mg XII	Si XIII	Si XIV	S XV
$\log T_{\max}$ (K)	6.60	6.80	6.90	7.00	7.20	7.20
λ_{lab} (Å)	13.4473	9.1687	8.4193	6.6479	6.1805	5.0387
λ_{obs} (Å)	13.454	9.175	8.419	6.650	6.181	5.038
Line flux	1.3 ^b	6.6	10.4	34.3	24.7	33.1
FWHM (mÅ)	[23] ^a	31 ± 9	27 ± 3	27 ± 3	23 ± 2	23 ± 3
FWHM (km s ⁻¹)	1014 ± 294	962 ± 107	1218 ± 135	1116 ± 97	1370 ± 179
G	0.8 ^{+0.4} _{-0.3}	0.9 ^{+0.5} _{-0.3}	...	0.8 ^{+0.4} _{-0.3}
R	3.7 ^{+1.8} _{-1.2}	1.8 ^{+0.9} _{-0.5}	...	2.5 ^{+1.2} _{-0.8}
R_0	3.6	2.7	...	2.6

NOTE.—All data are from HEG except Ne IX (MEG). λ_{lab} and T_{\max} are from APED. Absolute wavelength accuracy for λ_{obs} is ± 6 mÅ for HEG and ± 11 mÅ for MEG. Flux is the observed (absorbed) value after continuum subtraction in units of 10^{-14} ergs cm⁻² s⁻¹. Flux uncertainties are 20%. For He-like triplets (Ne IX, Mg XI, Si XIII), the quoted flux is for the resonance line only. $G = (f + i)/r$ and $R = f/i$. R_0 is the theoretical low-density limit at T_{\max} (Si and Ne are from Pradhan 1982; Mg is from Porquet et al. 2001).

^a The Ne IX r line is blended with Fe XIX (13.464 Å), so FWHM is not measurable and was held fixed at the MEG resolution of 23 mÅ during flux measurement. The observed flux has been decreased by 15% to account for the estimated contribution from Fe XIX.

mainly to solar abundance material in the O star wind (see also Willis et al. 1995). Global fits of the first-order MEG spectrum give an equivalent hydrogen column density $N_{\text{H}} = 2.2^{+0.1}_{-0.2} \times 10^{22}$ cm⁻² and a flux in the 0.4–10 keV range $F_{\text{x}} = 1.2$ (9.8) $\times 10^{-11}$ ergs cm⁻² s⁻¹, where the value in parentheses is unabsorbed. At $d = 258$ pc, the intrinsic (unabsorbed) source luminosity is $L_{\text{x}} = 7.8 \times 10^{32}$ ergs s⁻¹. The DEM model shows a strong emission measure peak near ~ 9 –10 MK. Our initial analysis suggests that the iron abundance is well below solar with inferred values in the range 0.13–0.33 solar, referenced to Anders & Grevesse (1989). This result is preliminary and will require confirmation in more detailed abundance modeling that accounts for the possible effects of resonant trapping (Stevens et al. 1996) and nonthermal line broadening (§ 3.3.2).

3.3.2. Emission-Line Properties

Table 1 summarizes the properties of the brightest emission lines. All measured quantities in Table 1 are from the HEG

spectrum except for the weak Ne IX triplet (Fig. 4), where MEG was used to improve the S/N. We find no evidence for Doppler shifts in the line centroids of any of the strongest HEG lines to within the absolute wavelength accuracy of HEG (± 6 mÅ). As Table 1 shows, the agreement between the measured Gaussian line centroids and their APED rest-frame values is considerably better than the formal ± 6 mÅ HEG accuracy, with offsets of only ± 2 mÅ for the brightest HEG lines. Not only are these offsets small, but there is no systematic shift toward the red or blue.

Line broadening is detected in the strongest HEG emission lines. Gaussian fits give FWHM values in the range 23–31 mÅ (Table 1), which are roughly a factor of 2 broader than the HEG instrumental resolution (12 mÅ FWHM) and a factor of ~ 5 broader than the thermal line widths. Although the lines are broadened, they do not obviously show the blueshifted asymmetries predicted for line formation in an outflowing wind (Owocki & Cohen 2001). A possible exception is Mg XII (8.4193 Å), which exhibits a blueward asymmetry in the HEG line profile but shows no Doppler shift in its emission peak (Table 1).

3.3.3. He-like Triplets

Helium-like triplets were detected in Si XIII (Fig. 3), Mg XI, and Ne IX (Fig. 4). Table 1 gives the observed flux ratios $G = (f + i)/r$ and $R = f/i$ for the resonance (r), intercombination (i), and forbidden (f) lines. The f line is substantially stronger than the i line ($R > 1$) in all three triplets.

The G ratio is sensitive to temperature, while R is sensitive to the electron density (n) and stellar UV radiation field (Gabriel & Jordan 1969). If ϕ is the photoexcitation rate from the $1s2s^3S_1$ f level to the $1s2p^3P_1$ i level, then $R = R_0/[1 + (\phi/\phi_c) + (n/n_c)]$, where ϕ_c and n_c are the critical photoexcitation rate and critical density (see Blumenthal, Drake, & Tucker 1972). If photoexcitation and collisions are both negligible, then $R \rightarrow R_0$ in the low-density limit.

We obtain $R \approx R_0$ for all three He-like triplets if the lines are formed near T_{\max} (Table 1). Only for Mg XI is there any evidence for a value of R that is less than R_0 . However, the observed difference of 30% could very well be due to uncertainties in our line flux measurements and to possible blending of the Mg XI i line with weak Ne X Lyman series lines (see Huenemoerder, Canizares, & Schulz 2001 for a discussion of

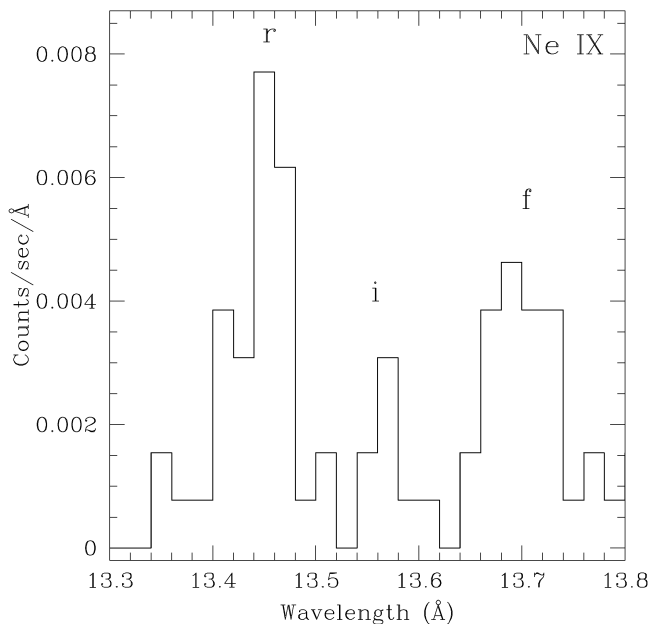


FIG. 4.—Ne IX triplet in MEG first-order binned at 0.02 Å

Mg XI blending issues). The G -values for Ne IX and Si XIII indicate that they are formed at temperatures near T_{\max} (Pradhan 1982). We thus conclude that *both* collisional excitation and photoexcitation are negligible in the regions where the Ne IX and Si XIII triplets are formed, implying $n \ll n_c$ and $\phi \ll \phi_c$. For Ne IX, $n_c = 6 \times 10^{11} \text{ cm}^{-3}$ (Blumenthal et al. 1972; Pradhan 1982) and the electron density is thus no larger than a few times 10^{11} cm^{-3} at $T \approx T_{\max}(\text{Ne IX}) = 4 \text{ MK}$.

The absence of a detectable photoexcitation effect in the observed R ratios provides useful constraints on the regions where the triplets are formed. Photoexcitation by the O star is of primary concern since a colliding wind shock is expected to form within $2R(\text{O})$ of the O star. Allowing for 20% line flux uncertainties, photoexcitation ratios $\phi/\phi_c > 0.5$ would have been unambiguously detected in the spectra as reduced ratios $R < \frac{2}{3}R_0$. The photoexcitation ratios ϕ_*/ϕ_c at the surface of the O star can be estimated by scaling the results in Table 2 of Blumenthal et al. (1972) to $T_{\text{eff}}(\text{O}) = 35,000 \text{ K}$ (De Marco & Schmutz 1999). We obtain $\phi_*/\phi_c = 10, 81, \text{ and } 853$ for Si XIII, Mg XI, and Ne IX, respectively, evaluated at $T = T_{\max}$ for a 35,000 K blackbody. Enforcing the observational constraint $R \geq \frac{2}{3}R_0$ (or equivalently $\phi/\phi_c \leq 0.5$) and applying a radiation field dilution factor $D(r) = 0.5\{1 - [1 - (R_*/r)^2]^{1/2}\}$ gives the following *minimum* line formation radii: $r_{\min} \approx 3R(\text{O}), 9R(\text{O}),$ and $30R(\text{O})$ for Si XIII, Mg XI, and Ne IX. If the triplets are formed at distances greater than these minimum radii, then O star photoexcitation will be negligible, consistent with the observed R ratios. These values of r_{\min} could be refined using sophisticated models for the winds and radiation fields of both stars. A smaller value of r_{\min} would be obtained for Si XIII by including the effects of $\text{Ly}\alpha$ absorption. However, the Ne IX $f \rightarrow i$ transition lies longward of $\text{Ly}\alpha$, and it is already clear that Ne IX is formed at distances of tens of stellar radii or more from the O star, not near its surface.

4. COMMENTS ON EMISSION MODELS

The γ^2 Vel spectrum shows heavy absorption, plasma temperatures ranging from ~ 4 to $\geq 25 \text{ MK}$, broadened unshifted lines that are approximately symmetric (Mg XII possibly ex-

cepted), and strong forbidden lines. These properties contrast sharply with the Doppler shifts and weak forbidden lines seen in the O4 I star ζ Pup (Cassinelli et al. 2001; Kahn et al. 2001). Instead, the broadened unshifted lines in γ^2 Vel and the presence of the high-temperature Fe XXV line more closely resemble the HETG spectrum of the young O7 V star θ^1 Ori C (Schulz et al. 2000). The heavy absorption and Fe XXV line seen in γ^2 Vel are not anticipated for radiative shocks, and the asymmetric blueshifted profiles predicted for line formation in an outflowing wind are not seen in our data. These results suggest that soft radiative shock emission, if present, is largely masked by the strong absorption.

Colliding wind shock models may provide a realistic description of the X-ray emission, but this remains to be demonstrated with synthetic spectra generated from hydrodynamics simulations. Such models must convincingly show that He-like triplets can form in a colliding wind shock in regions of low photoexcitation. Our analysis indicates that Ne IX is formed at distances of at least $\sim 30R(\text{O})$ from the O star, or about twice the orbital separation [$R(\text{O}) = 12.4 R_{\odot}$; De Marco & Schmutz 1999]. In γ^2 Vel, the W-R wind is dominant, and previous simulations suggest a rather narrow shock cone opening angle (Fig. 6 of Stevens et al. 1996). In such a geometry, lines such as Ne IX might be formed in cooler plasma well downstream of the O star where the wind velocity component perpendicular to the shock interface is reduced.

Numerical simulations will also need to demonstrate that a colliding wind shock can produce broadened emission lines without detectable Doppler shifts. This result is somewhat surprising given the high terminal wind speeds of $\sim 1550\text{--}2500 \text{ km s}^{-1}$ in γ^2 Vel. Accurate modeling of the viewing geometry will obviously be required. Even so, the upper limits on allowable Doppler shifts are quite stringent for the brightest lines (Table 1) and will place strict limits on line-of-sight velocities within the shock flow.

This work was supported by SAO grant GO0-1084X. We thank the members of the *Chandra* support teams and are grateful to K. Arnaud for assistance with HEASOFT.

REFERENCES

- Anders, E., & Grevesse, N. 1989, *Geochim. Cosmochim. Acta*, 53, 197
 Blumenthal, G. R., Drake, G. W., & Tucker, W. H. 1972, *ApJ*, 172, 205
 Cassinelli, J. P., Miller, N. A., Waldron, W. L., MacFarlane, J. J., & Cohen, D. H. 2001, *ApJ*, 554, L55
 De Marco, O., & Schmutz, W. 1999, *A&A*, 345, 163
 De Marco, O., et al. 2000, *A&A*, 358, 187
 Evans, I. 2001, *Chandra News*, 8, 13
 Gabriel, A. H., & Jordan, C. 1969, *MNRAS*, 145, 241
 Huenemoerder, D. P., Canizares, C. R., & Schulz, N. S. 2001, *ApJ*, in press
 Kahn, S. M., et al. 2001, *A&A*, 365, L312
 Lucy, L. B., & White, R. L. 1980, *ApJ*, 241, 300
 Owocki, S. P., & Cohen, D. H. 2001, *ApJ*, in press
 Porquet, D., Mewe, R., Dubau, J., Raassen, A., & Kaastra, J. 2001, *A&A*, submitted
 Pozzo, M., Jeffries, R. D., Naylor, T., Totten, E. J., Harmer, S., & Kenyon, M. 2000, *MNRAS*, 313, L23
 Pradhan, A. K. 1982, *ApJ*, 263, 477
 Prilutskii, O., & Usov, V. V. 1976, *Soviet Astron.—AJ*, 20, 2
 Schaerer, D., Schmutz, W., & Grenon, M. 1997, *ApJ*, 484, L153
 Schmutz, W., et al. 1997, *A&A*, 328, 219
 Schulz, N. S., Canizares, C. R., Huenemoerder, D., & Lee, J. C. 2000, *ApJ*, 545, L135
 Smith, R. K., & Brickhouse, N. S. 2000, *Rev. Mexicana Astron. Astrofis. Ser. Conf.*, 9, 134
 Stevens, I. R., et al. 1996, *MNRAS*, 283, 589
 Tokovinin, A. A., Chalabaev, A., Shatsky, N. I., & Beuzit, J. L. 1999, *A&A*, 346, 481
 Usov, V. V. 1992, *ApJ*, 389, 635
 van der Hucht, K. A., et al. 1997, *NewA*, 2, 245
 Waldron, W. L., & Cassinelli, J. P. 2001, *ApJ*, 548, L45
 Willis, A. J., Schild, H., & Stevens, I. R. 1995, *A&A*, 298, 549